

Field evolution of vortex lattice in $\text{LuNi}_2\text{B}_2\text{C}$ seen by decoration in fields up to 1.5 kOe

L.Ya. Vinnikov, T.L. Barkov

Institute of Solid State Physics, Chernogolovka, Moscow Region, 142432 Russia

P.C. Canfield, S.L. Bud'ko, and V.G. Kogan

Ames Laboratory DOE and Department of Physics, Iowa State University, Ames, Iowa 50011, USA

Evolution of the vortex lattice, the rhombus-square transition included, for $\text{LuNi}_2\text{B}_2\text{C}$ in the field along the c crystal axis, is tracked by the decoration technique pushed up to the record high (for this method) field of 1480 Oe. Decoration images are analyzed with the help of the Fourier transform, which indicates disordered structures in small fields of a few Oe. In fields $H < 200$ Oe the coexisting domains of different structures are observed. A technique based on the Fourier transform is employed to see the domains separately. The transition to the square lattice is recorded near 900 Oe. The results are in agreement with predictions of the nonlocal London theory.

PACS numbers: 74.60.-w, 74.60.Ec, 74.60.Ge

I. INTRODUCTION

The family of the rare-earth (R) metallic nickel-borocarbides $\text{RNi}_2\text{B}_2\text{C}$ has been the subject of considerable recent attention due to the interplay of magnetic and superconducting properties.^{1,2} The critical temperature T_c of these materials depends on the particular rare earth (or their combination), or on material purity, and ranges from zero to about 16 K in nonmagnetic members such as $\text{LuNi}_2\text{B}_2\text{C}$. The vortex lattices (VL) in these compounds exhibit a variety of phases with changing magnetic field and temperature. Studies of VL's are facilitated by availability of large high quality single crystals² with a relatively large Ginzburg-Landau parameter, $\kappa \sim 10 - 20$, low pinning, and a broad region of the HT phase diagram where the superconducting magnetic properties are nearly reversible.

The structural phase transition from the triangular to square VL driven by the magnetic field is of a particular interest. A variety of experimental techniques are used to study this transition: small-angle neutron scattering (SANS)³⁻⁵, scanning tunneling microscopy (STM)⁶, and Bitter decoration by small magnetic particles.^{3,7} The SANS and STM methods require rather high magnetic fields (few kOe and higher), whereas decoration is commonly employed for fields on the order of several hundred Oe or less because of a relatively low resolution.

For $\text{ErNi}_2\text{B}_2\text{C}$, the phase transition from the triangular to square VL in increasing field has been recorded by SANS and complemented by decoration.³ Decoration patterns revealed coexistence of the square and triangular lattices in fields near 600 Oe. In $\text{LuNi}_2\text{B}_2\text{C}$ crystals, the square vortex lattice for high magnetic fields of a few Tesla has been seen in STM.⁶ No experiments in low magnetic fields were carried out for this material. The theoretical model, which describes most of the features of evolving VL's is based on the London theory corrected for nonlocal effects.⁸

In this work the VL's in $\text{LuNi}_2\text{B}_2\text{C}$ were studied by the

decoration method. To cover the field range of greatest interest for the VL evolution, the method was extended up to fields of 1.5 kOe, the field region unprecedented for the decoration technique in materials with $\kappa \gg 1$. To our knowledge, the maximum field at which the decoration has been attempted was 1100 Oe on Nb.⁹

II. EXPERIMENTAL

We have used single crystals $\text{LuNi}_2\text{B}_2\text{C}$ of the size $\sim 3 \times 5$ mm in the ab -plane and ~ 0.5 mm thick. The crystals were grown from Ni_2B flux, as described elsewhere.^{2,10} Experiments were carried out in the field cooled regime with the field nominally parallel to the c axis (within a few degrees). For all fields except 1480 Oe, the temperature was set 4.2 K initially but may have risen to 7-9 K during the decoration experiment. For 1480 Oe, the initial temperature was 1.5 K. To minimize effects of inhomogeneities and pinning, decorations were done on a particular location of the same sample which was cleared by acetone after each decoration. A scanning electron microscope was used to resolve decoration patterns on the sample surface and to determine VL orientations relative to the crystal by comparing decorations with electron channeling patterns (ECP).

Routinely, the decoration experiments are done in fields near the lower critical field H_{c1} on samples as thin platelets in the perpendicular magnetic field. Since there is no quantitative theory to estimate the resolution limit, we use the following qualitative guidelines in pushing the method to higher fields:

1. The size of magnetic particles should be small relative to the London penetration depth $\lambda(T)$ and to the intervortex spacing $\sim \sqrt{\phi_0/B}$.
2. The density of particles should be small to avoid clustering.
3. The field gradients due to VL's should be large enough for the interaction with the particle magnetic mo-

ment μ to exceed the thermal energy, $\mu H > 3k_B T$.¹¹

The first condition is realized by manipulation of the buffer helium pressure within ≈ 0.1 torr. The optimal size of particles of 5 – 10 nm should not limit the resolution up to fields ~ 10 kOe. The second requirement is met by empirically minimizing the quantity of the evaporated magnetic material and by varying the distance between the heater and the sample. The most difficult to control and to satisfy is the last condition because the magnetic moment μ of iron particles is unknown. Besides, the actual temperature of decoration is uncertain because of the heating during the iron evaporation. Still, one has to keep this T as low as possible. To achieve this, we used onset temperatures 1.5 – 2 K for decoration in high fields. In this work, we have found that the contrast images of decorated VL's in $\text{LuNi}_2\text{B}_2\text{C}$ can be readily resolved in fields up to 1480 Oe.

The information one can extract from decoration experiments in fields below H_{c1} differs from the case $H \geq H_{c1}$. In the first case, the intervortex distance exceeds the penetration depth λ , and one can well resolve single vortices. However, the intervortex interaction in this situation is too weak to arrange vortices in a well ordered lattice, given the competition with disordering pinning. Nevertheless, one can utilize the decoration data to obtain a rough estimate of the penetration depth. The field distribution of a single vortex in the bulk has a characteristic diameter of 2λ . Near the sample surface the vortex field “opens up”.¹² As a result, the field gradients at the sample surface are lower than in the bulk. The field lines at a distance λ from the vortex core in the bulk, cross the surface at a larger distance from the core. One may consider the magnetic diameter of the vortex at the surface as $L \approx m\lambda$, where the empirical expansion factor m can be determined measuring the size L of the iron particle clusters forming at each vortex site during the low field decoration. Data show that $m \approx 4$ provides a good estimate of λ .

In applied fields well above H_{c1} , the fields of neighboring vortices overlap, and the resolution of decoration experiments drops. Nevertheless, the contrast of the decoration patterns still provides enough quantitative information on the VL symmetry and intervortex spacing. The computer processing of the images (fast Fourier transform and image filtering followed by inverse Fourier transform) greatly enhance our ability to study VL's and the domain structures in fields which were thought inaccessible to the decoration technique. In this work, VL's were successfully decorated and analyzed in a broad field interval from 4 to 1480 Oe.

III. RESULTS

As is seen in Fig. 1, in small fields vortices do not form a well ordered lattice. A straightforward count shows that the average intervortex spacing corresponds to one

flux quantum per vortex.

High magnification images of single vortices reveal the average size of the iron clusters of about 600 nm. Taking this as an estimate of 4λ at $T \approx 0.5T_c$, we obtain $\lambda_0 \approx 130$ nm utilizing the two-fluid approximation $\lambda^2(T) = \lambda_0^2/(1 - T^4/T_c^4)$. This value is larger than 71 nm obtained from the H_{c1} data,¹⁶ and ≈ 100 nm (Ref. 17) obtained from the magnetization measurements, but close to the estimate of Ref. 1.

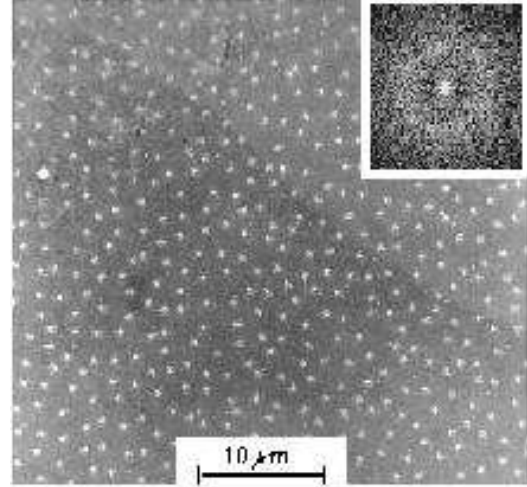


FIG. 1. Vortices in field $H = 4.5$ Oe along the c crystal axis. The Fourier transform in the inset indicates that the vortex system is an amorphous solid.

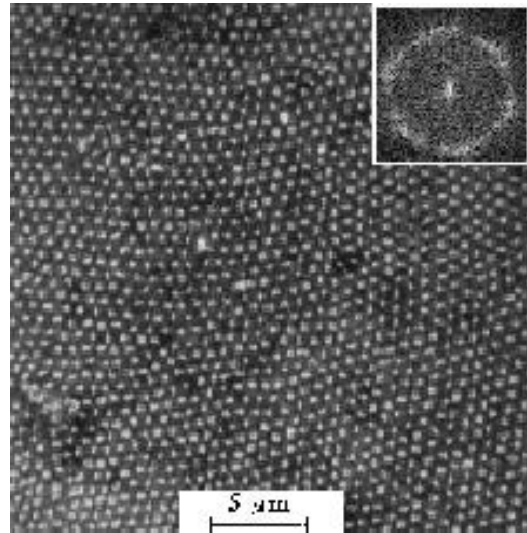


FIG. 2. Vortex system for $H = 40$ Oe. Domains of well ordered lattices are seen. The maxima of the Fourier transform are smeared due to varying orientations of the domains.

In higher fields, intervortex interaction is stronger and vortices form ordered lattices. Starting from ≈ 40 Oe and up to ≈ 200 Oe we observe domains of nearly regular tri-

angular VL's; see Fig. 2. VL orientations within each domain are quite random. Typical size of a domain is a few intervortex distances and increases with the magnetic field.

An example of VL at $H = 200$ Oe is shown in the upper panel of Fig. 3. The Fourier transform (FT) of this pattern shows that the structure consists of three nearly regular triangular domains with different VL orientations.

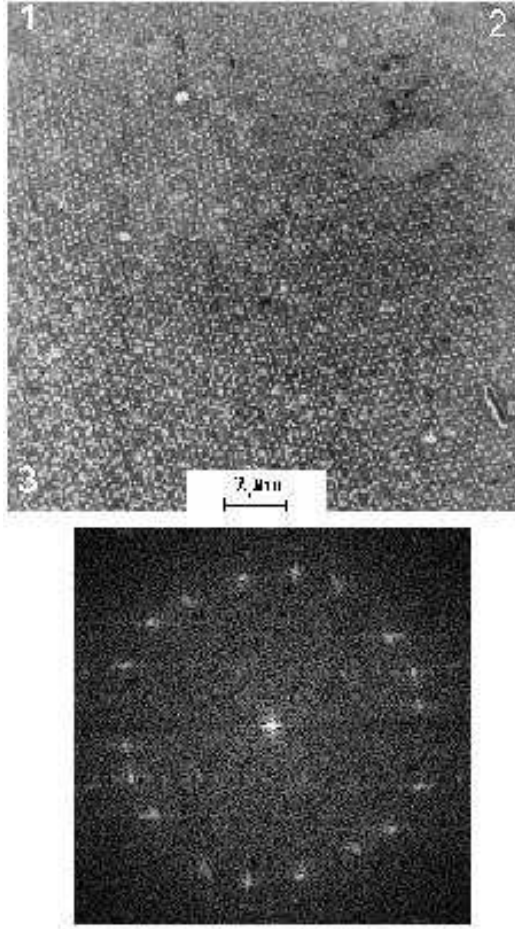


FIG. 3. The upper panel: the three-domain structure for $H = 200$ Oe. The domains (marked as 1,2,3) are shown separately in Figs. 4. The lower panel: Fourier transform of the upper panel pattern indicates the presence of three well ordered domains. Each of the domains is responsible for 6 maxima forming nearly a hexagon.

By choosing the FT maxima which belong to one of the domains and clearing all other reflexes one can obtain with the help of the inverse FT the patterns of all three domains in real space separately. These patterns are shown in Fig. 4.

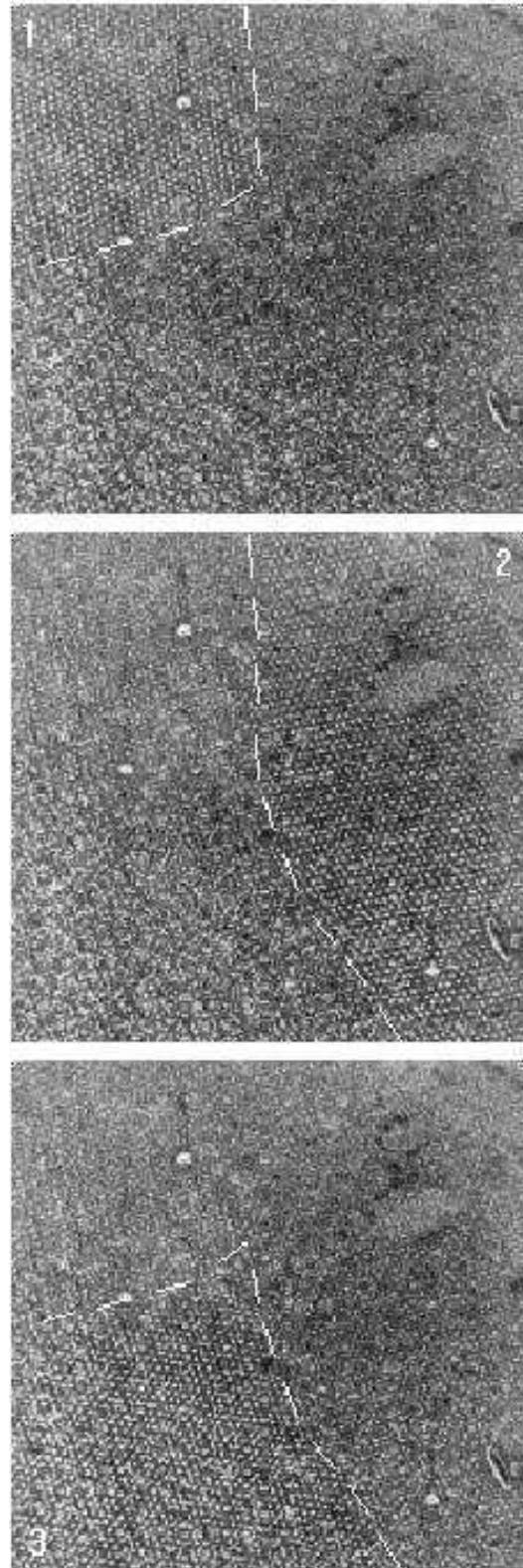


FIG. 4. The three panels show three different VL's. Each one is obtained by the inverse Fourier transform of a selected sets of six maxima out of 18 of Fig. 3.

Note that the domain size (in units of intervortex dis-

tance) for 200 Oe is large as compared to domains in the field of 40 Oe.

The influence of crystal inhomogeneities and anisotropy on the VL domain structure and ordering has been extensively studied for NbSe₂.^{13,14} The nonlocality brings a new complexity to the process of domain formation because VL's now depend on T, H and the local mean-free path.¹⁵ Comparing the ECP picture of Fig. 5 with Figs. 4, we find that one of the closepacked directions on the upper panel is aligned with $\langle\bar{1}10\rangle$ direction of the crystal, whereas that of the middle panel is aligned with $\langle110\rangle$. It is worth noting that the model of Ref. 8 predicts that the short diagonal of the rhombic VL cell in small fields should point in one of these directions.

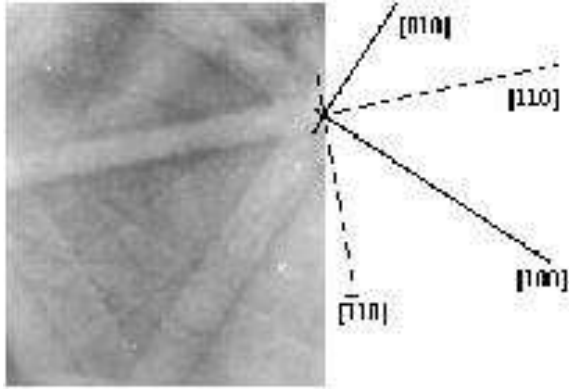


FIG. 5. Electron channeling pattern for the same place as the decoration of Fig. 3.

In fields more than 200 Oe, the typical domain size considerably exceeds the intervortex distance. The orientation of the closepacked VL direction in most domains correlates (within few degrees) with $\langle100\rangle$ crystallographic direction; this is seen in Fig. 6 in which the decoration pattern for $H = 300$ Oe and the ECP picture are provided.

Still, in other domains the closepacked direction coincides with $\langle110\rangle$, the fraction of which decreases with field and at $H = 600$ Oe reaches $\approx 1/3$. The VL unit cell is nearly rhombic with the apex angle β exceeding 60° , as can be extracted from the FT in Fig. 7. The angle β increases with field. The preferable orientation of the VL corresponds to the unit cell diagonal opposite to β being aligned with $\langle100\rangle$.

In fields of about 600 Oe and higher, in some surface locations we observe domains of the square VL, whereas majority of the domains contain strongly distorted triangular (or, better to say, rhombic) VL, see FT in Fig. 7. The fraction of domains with the square lattice increases with increasing field. A similar situation has been seen in SANS data on V₃Si, where the presence of domains was deduced from analysis of the scattering maxima.¹⁸ Here, we see the domains directly.

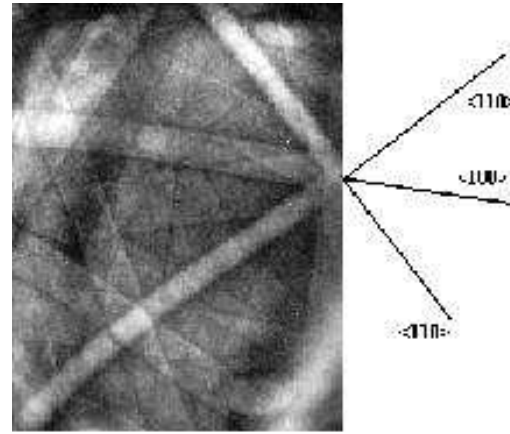
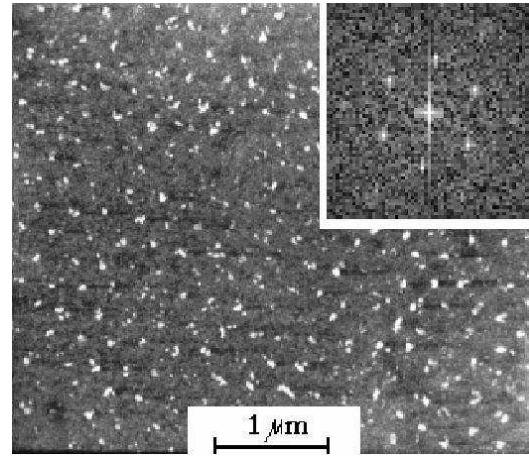


FIG. 6. The upper panel shows the decoration pattern for $H = 300$ Oe with the Fourier transform in the inset. The lower panel shows the corresponding electron channeling pattern indicating that one of the VL close-packed directions coincides with $\langle100\rangle$ crystal direction.

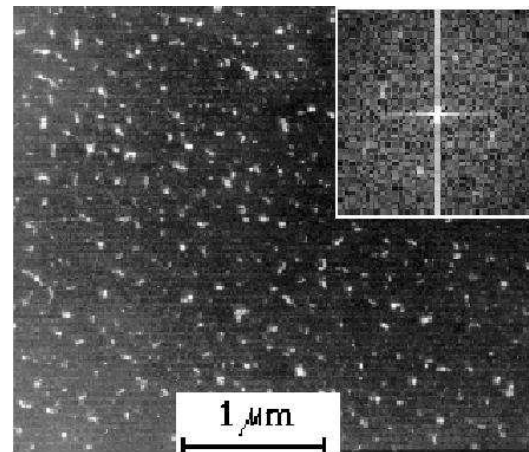


FIG. 7. The applied field is $H = 710$ Oe. The direction analysis of the Fourier transform in the inset gives $\beta \approx 82^\circ$ and the corresponding diagonal of the rhombic cell aligned with $\langle100\rangle$.

The square domains are dominant in fields of about 1000 Oe and higher, Fig. 8. The square diagonals are parallel to $\langle 100 \rangle$ and $\langle 010 \rangle$ crystallographic direction.

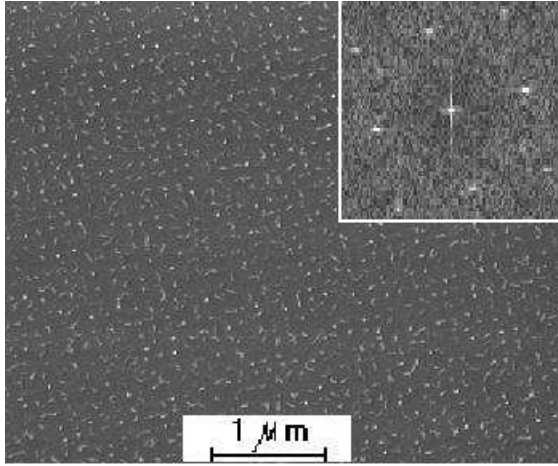


FIG. 8. The vortex lattice in the $\text{LuNi}_2\text{B}_2\text{C}$ single crystal for the field 1480 Oe parallel to the c axis.

The results of our study of VL's in $\text{LuNi}_2\text{B}_2\text{C}$ for a two particular locations on the crystal surface are collected in Fig. 9 where the field dependence of the angle β is shown. The triangles and circles show the decoration results from two different locations of the crystal. Few points for the same field indicate the scattering of the angle β within the decoration area of about $100 \times 100 \mu\text{m}$. In the field interval 200-600 Oe, the apex angle β of the rhombic unit cell slowly increases with field. With the further field increase, VL's deviate even faster from the standard triangular VL (with $\beta = 60^\circ$) toward larger

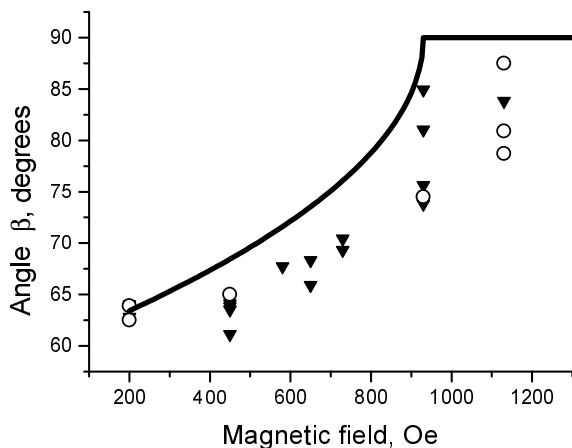


FIG. 9. The apex angle β versus H . The triangles and the circles are obtained at two different locations on the sample surface. A few triangles (circles) for the same field indicate that the data points are extracted from a few different locations of the same decoration patch.

IV. DISCUSSION

The theory of Ref. 8 predicts that in fields less than $H_1 \sim 200$ Oe along $\langle 001 \rangle$ crystal direction, the VL should have a rhombic unit cell with a short diagonal along either $\langle \bar{1}10 \rangle$ or $\langle 110 \rangle$. The apex angle β of the rhombus should be less than 60° . Experimentally, up to fields about 200 Oe we did not record a well ordered VL. Instead, a structure made of many domains with different lattice orientations is observed. The prediction for the value of $\beta < 60^\circ$ is also hard to verify in this field region.

One can argue that in small fields energy differences between different possible VL configurations are comparable with characteristic pinning energies. In this situation, the VL structure is affected by distribution of pinning sites which may vary throughout the sample. Therefore, we need better crystals of $\text{LuNi}_2\text{B}_2\text{C}$ to support or disprove the low field theoretical scenario for equilibrium VL's for this material (for $\text{YNi}_2\text{B}_2\text{C}$ this scenario has been confirmed⁵ by SANS data in fields up to 1200 Oe).

Still, the low field decoration results can be used to estimate the London penetration depth λ at decoration temperatures of $(0.3-0.5)T_c$. The value of λ obtained by measuring sizes of the particle clusters, is in a reasonable agreement with values obtained by other techniques.^{1,17} It is to be noted that λ estimated by measuring the "vortex diameter" d in decoration experiments is in a fair agreement with other data also for YBCO ,^{19,20} for which an empiric relation $d = 4\lambda$ yields $\lambda_0 \approx 150$ nm and for NbSe_2 for which the procedure gives ≈ 270 nm.²¹

With the magnetic field increasing, the role of pinning diminishes because the intervortex interactions become stronger. The field region with H exceeding approximately 300 Oe is more amenable for checking the theoretical model of Ref. 8. The model is based on the nonlocal London approach and as such requires a number of microscopic input parameters (the Fermi surface, the penetration depth, the mean-free path, to name a few) for a quantitative comparison with experiment. Here, we use a simpler "mean-field" approach based on the assumption that the structural transition from the rhombic to the square VL at the transition field we call H_2 is of the second order. This assumption is supported by numerical simulations of Ref. 8 which show that the rhombus-to-square transition at H_2 is accomplished by an infinitesimal deformation so that at the transition the structure changes continuously. Moreover, the square phase has an extra symmetry element: the 4-fold rotation axis which is absent in the rhombic cell. Both of these features are characteristic of a 2nd order transition. We, therefore, can apply the general Landau theory according to which the energy density near the transition at H_2 can be written as

$$F\{\eta; B\} = F_0(B) + a(B - H_2)\eta^2 + b\eta^4/2. \quad (1)$$

Here, F_0 is the part unrelated to the VL structure; the magnetic induction B for platelet-like samples is equal to the perpendicular applied field H . The field independent and positive coefficients a, b are related to a particular VL; η is a properly defined order parameter which should be zero in equilibrium above H_2 . Since the apex angle of the high-field structure is $\pi/2$, one can choose $\eta = \pi/2 - \beta$. Note that the field B in (1) plays the role of temperature in the standard Landau theory.

The equilibrium structure corresponds to $\partial F/\partial \eta = 0$ which yields $\eta = 0$ above H_2 and

$$\beta^{(1,2)} = \frac{\pi}{2} \mp \sqrt{\frac{aH_2}{b} \left(1 - \frac{B}{H_2}\right)}. \quad (2)$$

for $B < H_2$. The two signs correspond to two possible structures with apex angles $\beta^{(1)} + \beta^{(2)} = \pi$; these are rhombic VL's rotated relative to each other by $\pi/2$. We then expect $(\pi/2 - \beta) \propto \sqrt{H_2 - B}$ near H_2 . In fact, the numerical simulations show that with good accuracy this dependence holds all the way down to small fields where β should approach $\pi/3$, i.e., $\sqrt{aH_2/b} \approx \pi/6$. Thus, the apex angle β (in degrees) should satisfy an approximate relation

$$\begin{aligned} \beta &\approx 90^\circ - 30^\circ \sqrt{1 - B/H_2}, & B < H_2, \\ \beta &= 90^\circ, & B > H_2 \end{aligned} \quad (3)$$

in a broad field domain near H_2 . This formula is convenient for comparison with data since it contains only one fitting parameter H_2 . The solid line in Fig. 9 is calculated with the help of Eq. (3) with $H_2 = 930$ Oe.

There are few reasons for a considerable spread of β values shown in Fig. 9. Since the lattice should undergo restructuring during the cooling, the cooling rate may affect the resulting structure. The gas pressure may influence the actual decoration temperature since during the "evaporation" of iron particles the sample heats up and cools down with the pressure dependent rate. Clearly, the spread related to different loci is related to crystal inhomogeneities. Moreover, the nonlocal London model predicts⁸ and the data¹⁵ confirm that the transition field H_2 is sensitive to the crystal purity (*via* the mean-free path ℓ). Even weak inhomogeneities in ℓ within one decoration patch of $100 \times 100 \mu\text{m}^2$ may influence VL structures. As is seen from Eq. (3), $d\beta/dB$ diverges as $B \rightarrow H_2$, in other words, a small spread in values of H_2 may cause a considerable variation in β . This statement can also be formulated as enhanced "structural fluctuations" near the second order transition at H_2 . In fact, our data show that the β spread peaks in the field interval $700 - 1000$ Oe, i.e., just near H_2 .

ACKNOWLEDGMENTS

We thank N.S. Stepanov, L.G. Isaeva, D.K. Finnemore, and J.E. Ostenson for assisting in this work. L.V.

and T.B. acknowledge the support of Russian State Program "High-temperature superconductivity, Volna 4-Vin". The work of L.V. was funded by Russian State Contract 107-1(00)-P and in part by a COBASE grant of the National Research Council. Ames Laboratory is operated for US DOE by the Iowa State University under Contract No. W-7405-Eng-82.

-
- ¹ G. Hilscher and H. Michor, *Studies of High Temperature Superconductors*, ed. by A. V. Narlikar, Nova Science Publishers, New York, **28**, 241 (1999).
 - ² P.C. Canfield, P.L. Gammel, and D.J. Bishop, *Physics Today*, **51**, 40 (1998).
 - ³ M.R. Eskildsen, P.L. Gammel, B.P. Barber, U. Yaron, A.P. Ramirez, D.A. Huse, D.J. Bishop, C. Bolle, C.M. Lieber, S. Oxx, S. Sridhar, N.H. Andersen, K. Mortensen, and P.C. Canfield, *Phys. Rev. Lett.* **78**, 1968 (1997).
 - ⁴ M. Yethiraj, D.M.K. Paul, C.V. Tomy, and E.M. Forgan, *Phys. Rev. Lett.* **78**, 4849 (1997).
 - ⁵ D.M.K. Paul, C.V. Tomy, C.M. Aegerter, R. Cubitt, S.H. Lloyd, E.M. Forgan, S.L. Lee and M. Yethiraj, *Phys. Rev. Lett.* **80**, 1517 (1998).
 - ⁶ Y. De Wilde, M. Iavarone, U. Welp, V. Metlushko, A.E. Koshelev, I. Aranson, G.W. Crabtree, and P.C. Canfield, *Phys. Rev. Lett.* **78**, 4273 (1997).
 - ⁷ A.B. Abrahamsen, M.R. Eskildsen, N.H. Andersen, P.L. Gammel, D.J. Bishop, P.C. Canfield, *Bulletin of the American Physical Society*, March 1999, Atlanta, Georgia, **44**, No. 1, UC27.
 - ⁸ V.G. Kogan, M. Bullock, B. Harmon, P. Miranovich, L. Dobrosavljević-Grujić, P. Gammel, D. Bishop, *Phys. Rev. B* **55**, 8693 (1997).
 - ⁹ E.H. Brandt, *Rep. Prog. Phys.* **58**, 1465 (1995); see also E.H. Brandt and U. Essmann, *Phys. Stat. Sol. (b)* **144**, 13 (1987).
 - ¹⁰ B.K. Cho, P.C. Canfield, and D.C. Johnson, *Phys. Rev. B*, **52**, 3844 (1995); see also Ref. 2.
 - ¹¹ H. Trauble and U. Essmann, *Phys. Stat. Sol.*, **18**, 813 (1966).
 - ¹² J. Pearl, *J. Appl. Phys.* **37**, 4139 (1966).
 - ¹³ C.A. Bolle, F. De La Cruz, P.L. Gammel, J.V. Waszczak, and D.J. Bishop *Phys. Rev. Lett.* **71**, 4039 (1993).
 - ¹⁴ F. Pardo, F. De La Cruz, P.L. Gammel, C.S. Oglesby, E. Bucher, B. Battlogg, and D.J. Bishop, *Phys. Rev. Lett.* **78**, 4633 (1997).
 - ¹⁵ P.L. Gammel, D.J. Bishop, M.R. Eskildsen, K. Mortensen, N.H. Andersen, I.R. Fisher, K.O. Cheon, P.C. Canfield, and V.G. Kogan, *Phys. Rev. Lett.* **82**, 4082 (1999).
 - ¹⁶ H. Takagi, R.J. Cava, H. Eisaki, J.O. Lee, K. Mizuhashi, B. Batlogg, S. Uchida, J.J. Krajewski, W.F. Peck Jr., *Physica C, Superconductivity*, **228**, 389 (1994).
 - ¹⁷ V.G. Kogan, S.L. Bud'ko, I.R. Fisher, and P.C. Canfield, *Phys. Rev. B* **62**, 9077 (2000).
 - ¹⁸ M. Yethiraj, D.K. Christen, D.M.K. Paul, P. Miranovich, and J.R. Thompson, *Phys. Rev. Lett.* **82**, 5112 (1997).

- ¹⁹ L.Ya. Vinnikov, L.A. Gurevich, G.A. Emelchenko, Ya.A. Ossipyan, Solid State Comm., **67**, 421 (1988).
- ²⁰ M.R. Trunin, Journal of Supercond. **11**, 381 (1998).
- ²¹ M.V. Marchevsky, L.A. Gurevich, P.H. Kes, and J. Aarts, Phys. Rev. Lett., **75**, 2400 (1995).